Northern Arizona University

Wind Turbine Technical Report
Submitted to: US Department of Energy
April 5, 2017

Collegiate Wind Competition Team

Mechanical Engineering Team:

Melissa Hoover (Project Manager)
Jesus Bravo (Blade Design)
Joshua Danny (Brake Design)
Chase Donnell (Tower Design)
Brent McFarlane (Budget Liaison)
Rafeal Vera Jr. (Design & Manufacturing Lead)

Electrical Engineering Team:

Mary Koehler (Project Manager)
Jialin Min (Client Liaison)
Victor Rinaldi (Development Manager)
Yakun Qie (Resource Investigator)

Faculty Mentors:

David Willy (Co-PI and Mechanical Technical Advisor)
Karin Wadsack (Principle Investigator)
Venkata Yaramasu (Electrical Technical Advisor)

Table of Contents

1 Executive Summary 1
2 Technical Design 2
2.1 Design Objective 2
2.2 Static Performance and Aerodynamics Analysis 3
2.3 Mechanical Loads 4
2.3.1 Rotor Dynamics 4
2.3.2 Blade Analysis 5
2.3.3 Main Shaft Analysis 5
2.3.4 Mechanical Brake Dynamics 6
2.3.5 Mainframe 7
2.3.6 Tower 7
2.3.7 Results and Factor of Safety Summary 8
2.4 Design for Varying Wind Direction 9
2.4.1 Bearing Selection 9
2.4.2 Tail Vane Design Analysis 9
2.4.3 Tail Vane Dimensions 9
2.4.4 Force Analysis 9
2.4.5 Yaw System Design Conclusion 10
2.5 Electrical Design 11
2.6 Electrical Analysis 11
2.7 Controls Analysis and Software Documentation 12
2.8 Testing 15
2.8.1 Testing Results 15
2.8.2 Testing Plans 15
3 References 16
4 Appendix A: Exploded View-Mainframe Tower, Tail, and Yaw System 17
5 Appendix B: Exploded View-Hub, Brakes, Drivetrain 18
6 Appendix C: Shaft Analysis MATLAB Program, DE-Gerber Failure Criteria 19
7 Appendix D: Equations 20
8 Appendix E: Assumptions and Material Properties 21

List of Tables

Table 1: Blade Design Elements 3
Table 2: Rotor Dynamics Calculated Values 5
Table 3: Drivetrain Factors of Safety 8
Table 4: Expected Loads and F.O.S. 9
Table 6: Wind Moment Results 10

List of Figures

Figure 1: 2017 Tunnel Turbine Designs: A) 2016 B) 2017 2
Figure 2: Power Output vs Wind Speed 4
Figure 3: Cp vs Tip Speed Ratio 4
Figure 4: Blade FEA Results: A) Deformation B) Stress 5
Figure 5: Main-Shaft Dimensions (mm) 6
Figure 6: Drivetrain Configuration 6
Figure 7: SOLIDWORKS FEA: A) Stress Distribution B) Deflection Analysis 7
Figure 8: Supporting Tower: A) Stress Distribution B) Deflection Analysis 8
Figure 9: Yaw System Design 10
Figure 10: Power Converter Topology 12
Figure 11: Boost Converter Topology 12
Figure 12: High Level block diagram for ABC/αß control 13
Figure 13: Electrical One-Line Diagram 14
Figure 14: Control State Flow Chart 14
Figure 15: Mechanical Braking System 15

1 Executive Summary

Team NAU has accepted the challenge to design a small-scale wind turbine to compete in the US Department of Energy Collegiate Wind Competition (CWC). This year, the team iterated upon Team NAU's 2016 design, with a focus on components including high performance blades, an originally designed DC-DC Boost Converter, and both yawing and braking systems. Analysis software, tools, and design processes from the previous year were utilized; however, the final product was used as a benchmark to improve upon.

The design constraints were derived from the competition rules and include size, power, and safety requirements. Some of the requirements exclusive to this year's competition include yaw rates up to 180 degrees per second, braking on command and when disconnected from the load, and cut-in speed between 2.5 and 5 m/s. These became the starting point for Team NAU's CWC17 turbine design and the emphasis for the redesign of the previous system. After the focus was identified, the team began analysis on individual subsystems to complete these tasks. The electrical team began research into boost converter designs by simulating power converters, power transformations and various boost converter designs. The team then designed a test bench, which included a purchased vertical Permanent Magnet Synchronous Generator (PMSG) wind turbine, diode bridge rectifier, off-the-shelf DC-DC Boost Converter and load to test components and boost converter designs. The mechanical team iterated over the requirements and began their comprehensive design. The first component designed was the blades. The blade performance was evaluated using Q-Blade, in which airfoils, twist, and chord length could be manipulated and simulations could be run to find the approximate cut-in speed and power output using the blade design. The next subcomponent was the mechanical braking system. The goal of the brake design is to reduce the rotor RPMs to less than 10% of full performance at that wind speed, and if possible, to zero RPMs with the capability of rapid start up. Team NAU chose a brake design that utilizes a carbon fiber disc brake with aluminum calipers controlled by a solenoid linear actuator. The final subcomponent designed was the yawing system for varying wind direction. The team decided to equip the turbine with a two-bearing and tail vane yawing system. The tail vane utilizes the normal force provided by the wind to orient itself parallel to wind flow, and the bearings located within the tower allow the mainframe to rotate about its axis.

The following report gives further explanation and documentation of Team NAU's design for the 2017 Collegiate Wind Competition. Analyses included are static performance and aerodynamics, mechanical load and safety factors, design for varying wind direction, electrical design and simulation, controls and software, and field-testing. Special acknowledgements to ***W.L. Gore and Associates*** for their financial donating as well as Michael and Justin Clifton at ***ARE Telecom and Wind*** for providing testing facilities.

2 Technical Design

2.1 Design Objective

The design objective for Team NAU for the 2017 Collegiate Wind Competition (CWC) was to iterate upon Team NAU's design for the 2016 competition. Last year's design included carbon fiber blades and a simply designed drive system with no yaw system. Additional competition tasks were added for this year's competition, which include safety tasks that require the turbine to stop on command and when disconnected from the load as well as durability tasks that require the turbine to remain oriented in the direction of yawed wind flow. These competition tasks defined the technical design requirements for the iterated turbine design. A few of the major requirements include: high power output, low cut-in speed, durability, safety, yawing, braking, minimal deployment time, and compact size. Team NAU's 2016 tunnel turbine design can be compared to the iterated 2017 tunnel turbine design in **Figure 1**. Full Exploded views of Team NAU's 2017 design can be found in Appendices A and B. The full list of technical design constraints for this year's design is listed below:

- Maximum wind speed of 18 m/s
- Yaw rates up to 180°/s
- Generate 10W between 5 to 11 m/s
- Supply a Load System
- Rotor dimensions less than 45 cm^3
- Non-rotor turbine parts fit within 15 cm diameter cylinder
- Rotor center within 2.54 cm of tunnel centerline
- Mountable within wind tunnel
- Base plate no thicker than ½ inch
- Turbine fits through the turbine door
- Maximum output voltage 48VDC at PCC
- No batteries
- Wiring and connectors for PCC and kill-switch
- Zero energy at the start of the test
- Bulk energy storage is safe
- Power fluctuation ± 10% for any 5s interval
- Cut-in speed less than 5 m/s

A **B**

***Figure 1**: 2017 Tunnel Turbine Designs: **A**) 2016 **B**) 2017*

2.2 Static Performance and Aerodynamics Analysis

Blades were designed to have low cut-in speed, to have high power output, and to be structurally sound based on a four-blade rotor. Blade shape was originally designed using Blade Element Momentum theory (BEM) and MATLAB. BEM requires inputs of Reynolds numbers, blade length, number of blade elements, tip speed ratio, and wind speed.

The Reynolds numbers for the blades were relatively low compared to those for industrial blades, so thin airfoils with high camber were chosen. Reynolds numbers for cut-in and rated speeds were 4,000-17,000 and 8,000-33,000 respectively. NACA airfoils were created to fit the requirements on thin airfoils with high cambers, and the airfoils tested were NACA 4402, 4605, 6715, 4404, 3408, 9422, 9620, also S1223 and Miley M06-13-128. These airfoils allow for lower cut-in speeds and higher power outputs for the small-scale blades. Analyses were ran for each airfoil using the blade analysis program Q-Blade, for the different Reynolds numbers along the chord length of the blade element. The resulting lift and drag ratios associated with different angles of attack were evaluated to select the airfoils with the ideal angles of attack. The final selected airfoils were NACA 4404, NACA 4605, and NACA 3408. Thinner airfoils were selected at first, but after 3D printing prototype blades it was apparent that the airfoils needed to be thicker to be more structurally sound. After airfoils selection, blade analysis was conducted on Q-Blade.

Blade chord length, twist, and airfoils were used in the blade analysis in Q-Blade; chord lengths and twists were gathered from the BEM calculations. 77 iterations were performed in Q-Blade that adjusted chord length, twist, and placement of the selected airfoils until a blade was created that met cut in and power requirements. The final blade properties are listed in **Table 1**. Although the team is concentrating efforts into the four-blade system, the team has also designed a simple three-blade rotor using only the NACA 4402 airfoil throughout the blade for contingency; however, the primary analysis focuses on a four-blade rotor design.

Table 1*: Blade Design Elements*

Current Blade Design			
Blade Position (mm)	**Chord (mm)**	**Twist (degrees)**	**Airfoils**
0	90	55	NACA 4404
19	76	47	NACA 4404
38	62	43	NACA 4404
57	55	37	NACA 4404
76	42	25	NACA 4605
86	37	17	NACA 4605
95	32	10	NACA 4605
114	29	6	NACA 3408
133	25	4	NACA 3408
144	24	2	NACA 3408
152	23	0	NACA 3408
170	20	-4	NACA 3408

Q-Blade analysis shows that the turbine will produce 17 watts of power at a wind speed of 10 m/s and a maximum power output of around 125 watts for higher wind speeds. However, this does not reflect actual power generation as the electronic and the mechanical losses are not accounted for in Q-Blade analysis. Cut-in speed is estimated at 3 m/s by comparing the output torque of the blades and the cogging torque of the generator. Figure 2 shows power output vs wind speed and Figure 3 shows coefficient of

performance vs tip speed ratio. Coefficient of power helps display how much of the available wind power the turbine is extracting, showing that the blades are working efficiently.

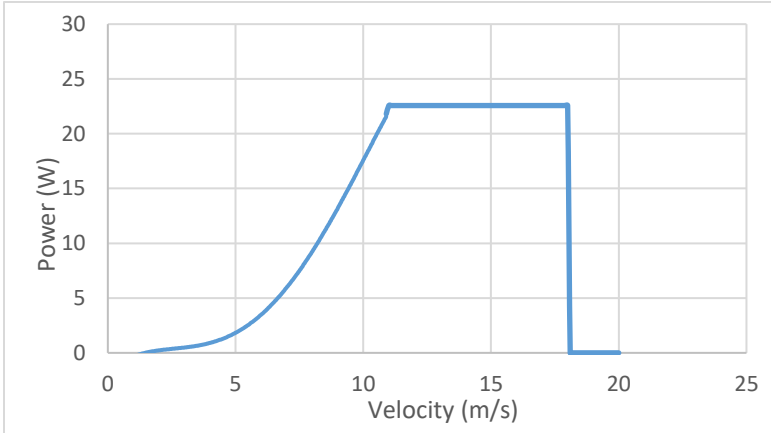

***Figure 2**: Power Output vs Wind Speed*

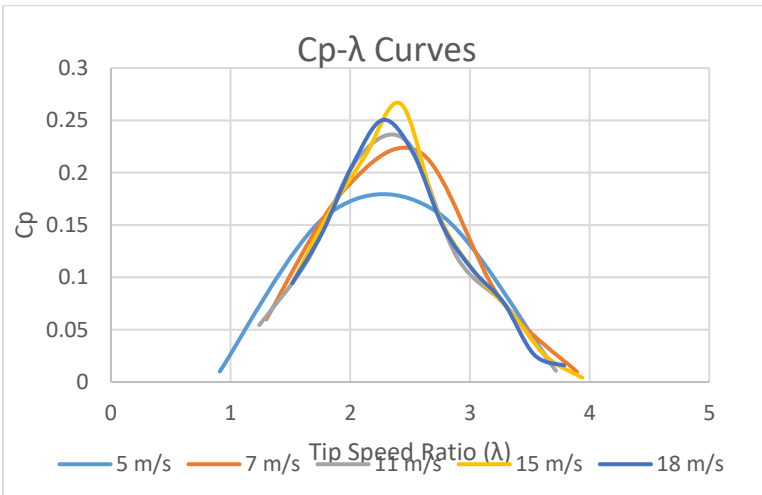

***Figure 3**: Cp vs Tip Speed Ratio*

2.3 Mechanical Loads

The effect of wind loads imposed on critical components such as the blades, main shaft, braking surfaces, support tower, and mainframe were analyzed for failure due to stress. A combination of SOLIDWORKS finite element analysis (FEA) and manual analysis were employed to refine each component for durability.

2.3.1 Rotor Dynamics

The blade rotor design consists of two separate configurations: three-blade and four-blade rotors. The rotors have similar designs and consist of a thrust washer and a hub which is mounted onto the main-shaft. The resultant rotor force from the four-blade rotor, F_R, generated by the centrifugal forces was used to estimate reactions for the drivetrain assembly. Centrifugal forces were also incorporated into the blade stress analysis. Direct thrust forces were incorporated into blade, mainframe, and supporting tower analyses but were assumed negligible on other non-rotor components due to compressive loading. Rotor torque was calculated for an ideal rotor using a conservative Coefficient of Performance of 0.500 and the Tip Speed Ratio of four. The resulting values for these analyses are listed in **Table 2**.

***Table 2**: Rotor Dynamics Calculated Values*

Property	**Calculated Value**
Actual Total Hub Mass	m_{HB} = *0.180 kg*
Analysis Total Hub Mass	m_{HB} = *0.305 kg*
Wind Speed	v_w= *18 m/s*
Estimated Maximum RPM	*n =6000 RPM's*
Estimated Maximum Torque	*Q = 0.200 N-m*
Thrust Force	F_T = *20 N*
Resultant Rotor Force	F_{Ry} = *3 N*

2.3.2 Blade Analysis

Blades were analyzed for yielding and deformation. The blades are manufactured using VEROCLEAR 3D printing filament that has an approximate yield stress of 50 MPa. Due to material flexibility, SOLIDWORKS FEA was used to determine stress factors of safety and deflections. The results of these analyses are shown in Figure 4. Forces considered include: centrifugal force, braking torque, and thrust force due to wind. Each blade was analyzed at a rotational speed of 6000 RPM with a torque of 0.250 Nm and a total thrust force of 20 N acting as a distributed load throughout each blade with majority of thrust applied at the blade tips. Four blade iterations were made to increase the factor of safety, clearance between mainframe components, and printing quality. The final blade design employs a thick blade root that decreases localized stress and deflections. The final blade design has a factor of safety of 1.35 and a maximum deflection of 6mm.

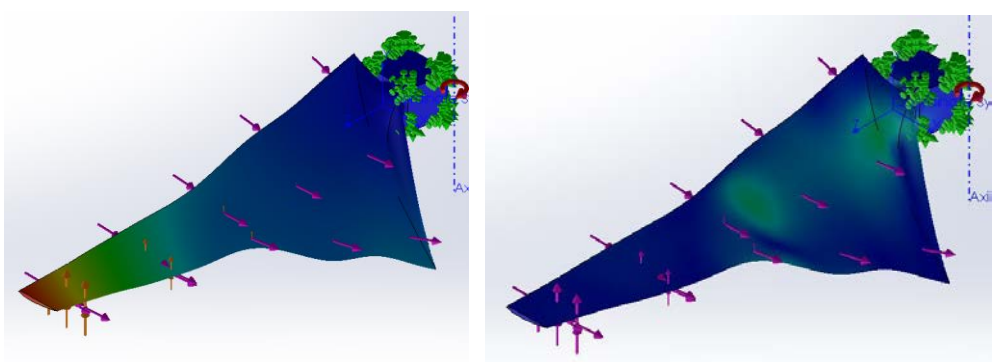

A **B**

***Figure 4**: Blade FEA Results: **A**) Deformation **B**) Stress*

2.3.3 Main Shaft Analysis

The resultant rotor force, F_R, was used to estimate reactions. The main shaft was modeled as a simply supported shaft with reaction forces at the rotor, bearing, and brake. The resulting reactions were 3N at the rotor, 5N at the main bearing, and 2N at the generator.

Since the reaction at the generator location was small, the bearing load at the generator was modeled at the end of the main-shaft assembly. The resulting torque was amplified by a compensation factor of two that accounts for rotational inertia. A shaft with initial estimated dimensions was iterated based on fatigue and static loading calculations using the DE-Gerber Failure Criteria shown in Appendix C. A MATLAB program was used to quickly calculate the shaft factors of safety for fatigue and static yielding, n_f and n_y. The material for the driveshaft is 7075-T651 Aluminum. Critical locations were identified where large stress concentrators were present. The main-shaft dimensions for the final iteration with final reactions are shown in Figure 5.

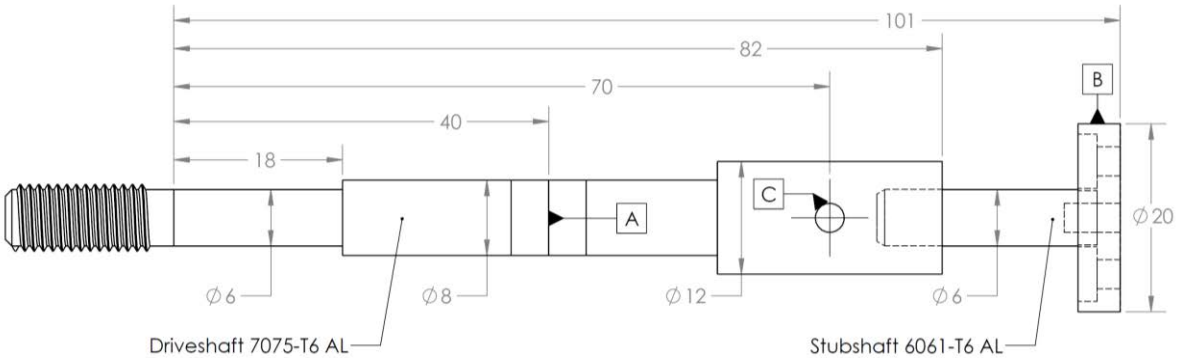

***Figure 5**: Main-Shaft Dimensions (mm)*

The bearing supporting the main-shaft at A has a maximum dynamic load rating of 2550N, is flange mounted and is self-aligning to +/- 5 degrees to account for shaft misalignment during assembly. The maximum dynamic load for each of the two bearings inside the SunnySky x4108s-380kV generator is 714N.

To facilitate manufacturing and to have a high level of concentricity, the final main-shaft design incorporates a two-piece assembly consisting of a stub shaft and driveshaft. The stub shaft is made of 6061-T6 Anodized Aluminum and is threaded into the driveshaft. Torque is transferred between the driveshaft and stub shaft through a jam nut. The flange on the stub shaft is attached to the generator with screws using the generator's factory mounting recommendations. A through hole at location C transfers torque from the driveshaft to the brake hub via steel torque screw. The final dimensions and factors of safety of the main-shaft assembly satisfy the goal of providing a lightweight, strong, and easy to assemble means of torque transfer.

2.3.4 Mechanical Brake Dynamics

The driving constraint for the driveshaft was to incorporate a powerful and reliable mechanical braking system. Other design constraints included: mass, failsafe capabilities, generator magnetism, and size. A carbon fiber brake disk with aluminum friction brake pads was selected to satisfy these constraints. The material combination decreases the rotational mass of the driveshaft, allows for large braking pressures, eliminates ferrous brake debris, and reduces the brake system size. Material properties are listed in Appendix E. Torque is transferred from the main-shaft to a 6061-T6 Aluminum brake hub through a torque screw. Torque is transferred from the brake hub to the brake disk through a hexagonal interface. The layout of the brake and drivetrain configuration is shown in **Figure 6**.

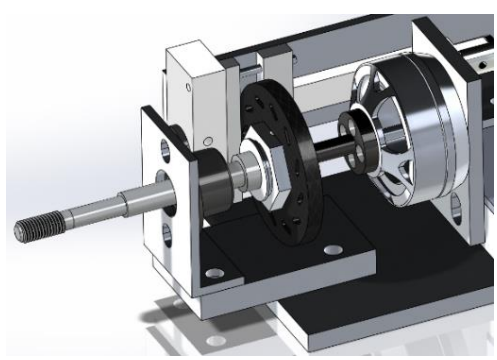

***Figure 6**: Drivetrain Configuration*

Using the equations found in Appendix D, brake force was estimated to be 55 N. However, the force is applied gradually using a spring to prevent shock to the blades. Brake force is adjusted by substituting

different springs with an actual applied force between 20 to 30 N. The maximum interface pressure between the brake disk and pads is 0.1837 MPa. To increase braking capacity and add modulation for RPM control, the dynamic brake from the previous turbine system is used in conjunction with the mechanical brake system to achieve satisfactory requirements.

2.3.5 Mainframe

The mainframe was designed to provide a rigid mounting platform for critical components to facilitate assembly. The mainframe consists of a 6061-T6 aluminum base plate and a 6061-T6 aluminum bearing flange that are welded together. A static SOLIDWORKS FEA analysis was performed with a distributed thrust load of 20N on each component face that is normal to wind direction. Results for stress distribution and deflection are shown in **Figure 7**. The resulting maximum stress was 9.16 MPa and the maximum deflection was 0.097 mm.

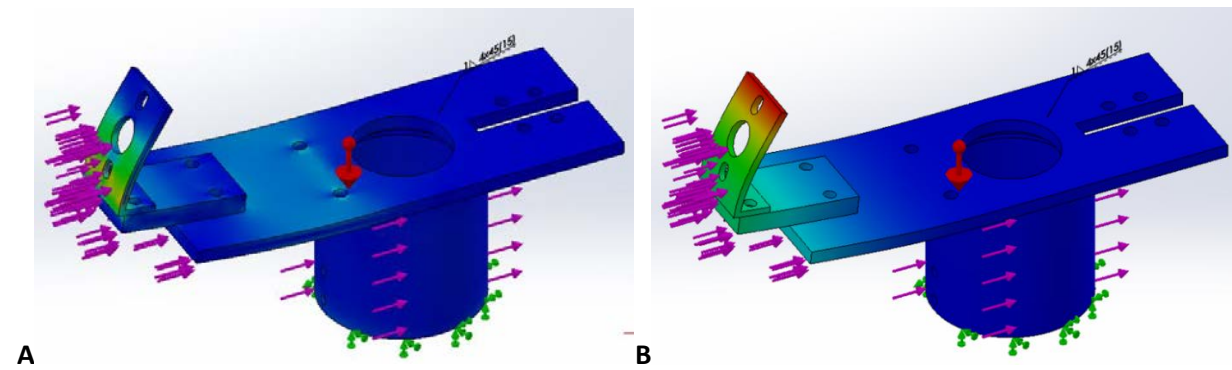

***Figure 7**: SOLIDWORKS FEA: **A**) Stress Distribution **B**) Deflection Analysis*

All mechanical turbine components are bolted onto mainframe. Interfaces between the mainframe and directly attached components compress thin rubber gaskets to reduce vibrations. Components mounted on the mainframe are aluminum to achieve an ideal weight distribution for yawing, with a center of gravity located above the center of rotation.

Yaw bearings are mounted inside the bearing flange with a near clearance fit for ease of assembly. The inner race of the bearings are mounted to the top of the supporting tower with an intermediate fit.

2.3.6 Tower

The tower must withstand the combined mechanical and thrust loads form the turbine components. The tower shaft was machined from A513 thick-walled mild steel tubing. The robust design accounted for freedom for machining steps for bearing mounting during the design phase. The tower shaft was welded to a A513 mild steel base plate. Thrust forces and gravitational loads were used to analyze stress at the weld and deformation at the upper section. Since the weld is much stronger than the material itself, the yield strength of A513 mild steel is used to calculate a conservative factor of safety. The stress distribution and deflections of the tower are shown in Figure 8. The maximum stress at the weld is 6.50 MPa and the maximum deflection of the tower is 0.075 mm.

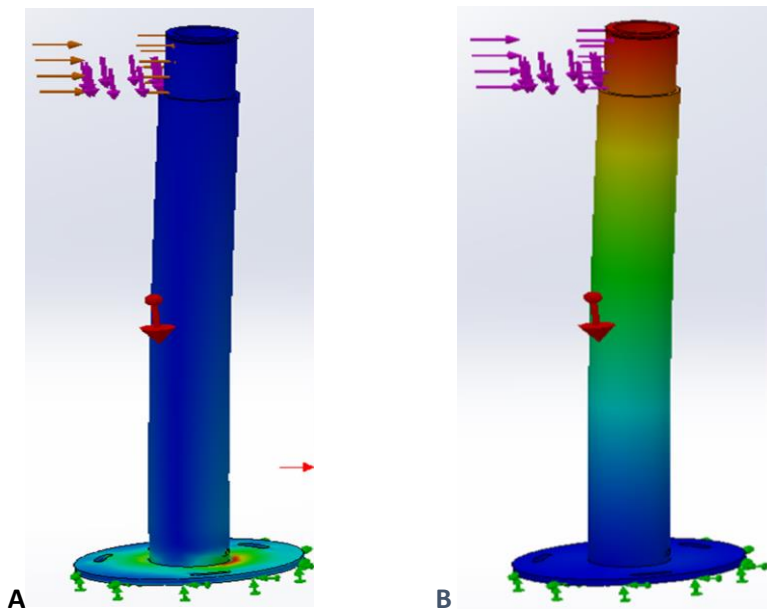

***Figure 8**: Supporting Tower: **A**) Stress Distribution **B**) Deflection Analysis*

2.3.7 Results and Factor of Safety Summary

Essential turbine components were analyzed for excessive stress and deformation to ensure the durability of the turbine. The resulting factors of safety (F.O.S.) for fatigue, static, and bearing dynamic loads for critical displacements along the drivetrain shaft as well as the alternating bending moments ($\mathrm{M_a}$) and mean torque ($\mathrm{T_m}$) at each of these locations are listed in Table 3 with reference to the main-shaft in Figure 5 with the datum at the left end of the main-shaft. The expected loads and factors of safety for crucial components are listed in Table 4.

***Table 3**: Drivetrain Factors of Safety*

Displacement	**18 mm**	**40 mm**	**70 mm**	**80 mm**
Dynamic Loads	M_a= 54.0 N-mm T_m = 375 N-mm	M_a= 120 N-mm T_m = 375 N-mm	M_a= 62.0 N-mm T_m = 375 N-mm	M_a= 38.0 N-mm T_m T_m= 375 N-mm
Fatigue F.O.S., n_f	n_f = 24.91	n_f = 46.05	n_f = 96.79	n_f = 13.44
Static F.O.S., n_y	n_y = 27.45	n_y = 61.66	n_y = 102.05	n_y = 13.39
Bearing Dynamic F.O.S.		n_A = 510		n_B = 714

***Table 4**: Expected Loads and F.O.S.*

Component	Material	Minimum FOS	Expected Loads	Load Description
Blades	VEROCLEAR 3D Filament	1.35	F_T = 20 N ω = 628 rad/s	Thrust Force, Centrifugal Force Brake Torque
Main-Shaft	7075-T6 and 6061-T6 Aluminum	13.39	R_{Ay} = 5 N M_a= 120 N-mm T_m = 375 N-mm	Max Reaction Force, Bending Moment, Mean Torque
Brake Assembly	6061-T6 Aluminum and Carbon Fiber Composite	13.60	F_B = 55N T_B = 375 N-mm p_{max} = 0.183 MPa	Braking Force, Braking Torque, Max Interface Pressure
Mainframe	6061-T6 Aluminum	30.00	$F_{T,D}$ = 20 N	Distributed Thrust Force
Tower	A513 Mild Steel	85.67	$F_{T,D}$ = 20 N F_M = 20 N	Distributed Thrust, Gravitational Load

2.4 Design for Varying Wind Direction

The turbine utilizes a passive yaw design to reduce the complexity of the system. This section covers aspects of the yaw design including bearing selection and loading as well as tail vane dimensioning and force analysis. Once these key factors were determined, they were evaluated to design an effective yawing system.

2.4.1 Bearing Selection

Bearing selection was dependent on the axial load due to the mass of the components that the bearings support. The mass of the upper turbine assembly was calculated by combining the mass of every component that is mounted to the mainframe. The total supported mass (hardware estimations included) is approximately 2 kilograms with a resultant force of 20N. From the selected bearing specification sheet, each bearing can withstand a static loading of 10.8 kN [8] and an axial load of one-fourth of the static loading value [9]. The maximum axial loading of each bearing becomes 2.7 kN. At this rating each yaw bearings has a factor of safety greater than two hundred.

2.4.2 Tail Vane Design Analysis

A main component for the passive yaw system is the tail vane that utilizes wind force to rotate the turbine about its axis until it is parallel with the wind. The analysis in this section determines the optimal tail vane design for successful tracking. The material selected for the tail vane was acrylic plexiglass. This material was chosen because of its durability, ease of manufacturing, and density required to balance the turbine's center of mass.

2.4.3 Tail Vane Dimensions

The surface area of the tail vane needed to be large enough to generate normal pressure adequate for the yawing moment required for wind tracking. The necessary surface area was calculated by multiplying two times the blade length squared, then dividing by 40 [1]. Using this formula, the necessary tail surface area was determined to be 32.4 cm^2.

2.4.4 Force Analysis

A force analysis was completed to determine if the selected tail vane design was sufficient to yaw the turbine into the wind. The two deep groove ball bearings in the tower create frictional resistance that the yawing moment must overcome. The combined frictional moment for both bearings was 0.001 N-m. The

frictional moment of the bearings was compared to the yawing moment, which was calculated using the force of the wind. To replicate a worst-case scenario, a wind speed of 2.5m/s was used to evaluate the yaw performance at the lower limit of the cut in speed.

Wind does not always contact the tail vane perpendicularly, but rather at an angle (Θ) which is defined as the yaw error. The cosine of this angle yields the component of the wind normal to the tail vane. Multiplying this by the force of the wind and the length of the moment arm gives the yaw moment. To maximize turbine performance, a maximum yaw error of 5° was desired, establishing the angle, Θ, used in this calculation.

After estimating the required surface area using a triangular model, it was determined that the area was not adequate to generate sufficient force to yaw the turbine efficiently. The surface area was then increased to 320 cm^2 and the new the factor of safety (F.O.S.) increased to above five. Using these values, the wind force was calculated to be 0.25 N. The final tail vane design was modified for aesthetics to replicate the shape of an axe blade to resemble Northern Arizona University's Logo. Although not triangular, the final shape provides the similar surface area of 290 cm^2 with comparable results. Table 5 shows the results of the wind force on different tail vane sizes with the final design denoted in blue.

***Table 5**: Wind Moment Results*

Tail Vane Size (cm^2)	Wind Force (N)	Yaw Moment (N-m)	Bearing Resistance (N-m)	F.O.S.
40	0.03	0.0007	0.001	0.7
320	0.25	0.0055	0.001	5.5
290	0.22	0.0050	0.001	5.0

2.4.5 Yaw System Design Conclusion

The yaw system analysis ensures the design of a reliable yaw for the turbine system. The final design yields better results than the initial surface area analysis used to find the minimum area required to rotate the turbine. The required surface area was increased to provide a larger force for a more reliable yaw. The tail vane design and yawing components are shown in **Figure 9**.

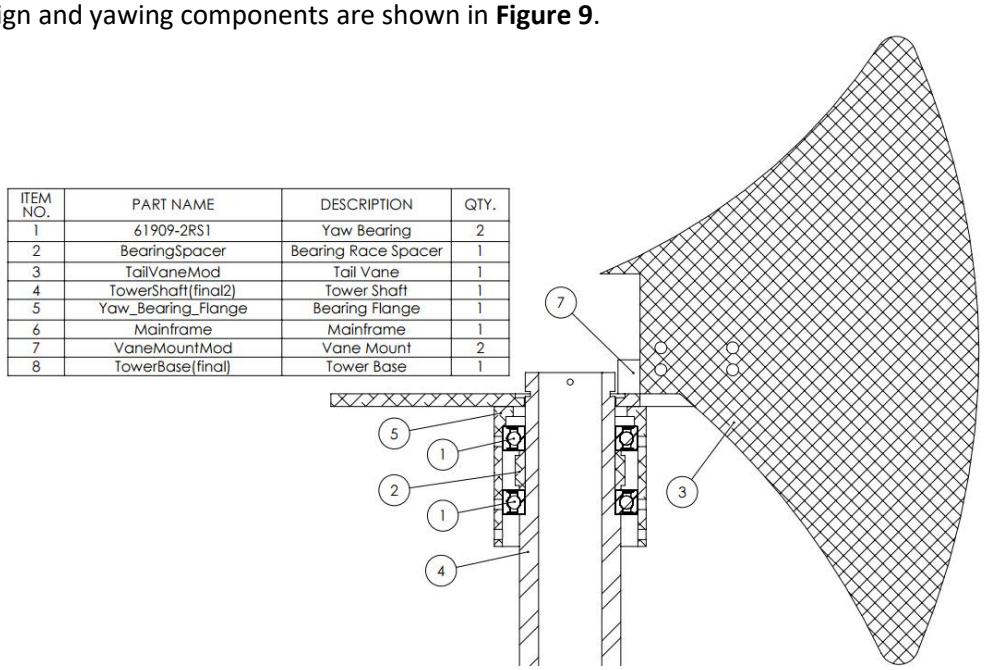

***Figure 9**: Yaw System Design*

2.5 Electrical Design

To test various off-the-shelf diode bridge rectifiers and boost converters, the Electrical team built a test bench to be used until the Mechanical team completed the working prototype of the wind turbine. A low power 75 W vertical wind turbine was purchased and mounted to a secure base. The three phase power wires were connected to a bread board for easy connection to various diode bridge rectifiers, boost converter designs, and a voltage regulated resistive load at 6V, 9V or 12V.

Two diode bridge rectifiers were tested with the test bench. One was made with six Schottky diodes and the second was IXYS FUS45 three phase AC-DC Rectifier. Six diodes were used because two diodes are required for passive rectification for each phase. Upon testing with the purchased wind turbine, the IXYS rectifier experienced smaller losses and preformed more efficiently than the other rectifier by 0.5 – 1V. The IXYS was then used to develop a separate rectifier board, which included a smoothing capacitor, bleed off resistor and heat sink. The heat sink was added to increase heat dissipation from the rectifier, increase efficiency, and avoid damage to components from excessive heat. It was then soldered to a printed circuit board (pcb) in preparation for future components.

Two off-the-shelf boost converters and one boost/buck converter was purchased and tested with the test bench to evaluate performance and observe difference in parts utilized in the design and research topologies. All three boost converters operated similarly and none of them performed better than the others with various load values. These boost converters were used as models for the final original design developed by the team. The parts used in these models were researched thoroughly and similar parts were purchased for the design.

Five Arduino Micro boards were purchased and programmed to control the regulated switching component of the original boost converter designed by the team. The microcontroller is passed in voltage and current levels from the boost converter and uses an OTSR Maximum Power Point Tracking algorithm to determine the reference variables needed to calculate the duty cycle of the switching component. The PID controllers needed to produce the reference current variable and duty cycle were programmed using Arduino's PID and PID Tuning libraries.

2.6 Electrical Analysis

Electrical Analyses were completed to confirm that the power circuit and its components met the expectations and requirements of the client.

The Arduino Micro microcontroller was programmed with the switch control algorithm with various switching frequencies to test the reliability of the microcontroller and confirm the effects on the circuit output. The MOSFET switching components were chosen over IGBTs because of their small current tail, optimizing performance in low-power applications. In the circuit testing stage, a MOSFET transistor replaced the boost converter diode to increase efficiency. Upon analysis, this synchronous boost converter configuration only increased efficiency by roughly 2%, but caused latency in the changes in the microcontroller duty cycle. The synchronous boost converter design was discarded. Silicon Carbide (SiC) Schottky Diodes were selected for the boost converter diode because of their low forward voltage and forward current. The forward voltage was measured to confirm the catalog ratings. No further relevant analysis was conducted. To minimize power dissipation in the circuit, the boost converter inductor value was minimized and the capacitor value was maximized within the bounds calculated by the team.

The final power circuit solution with the rectifier-board, OTSR controlled boost converter, and voltage regulated resistive load was tested along a spectrum of off-the-shelf turbine outputs and yielded an efficient and smooth power curve. The final circuit topology can be observed in Figure 10.

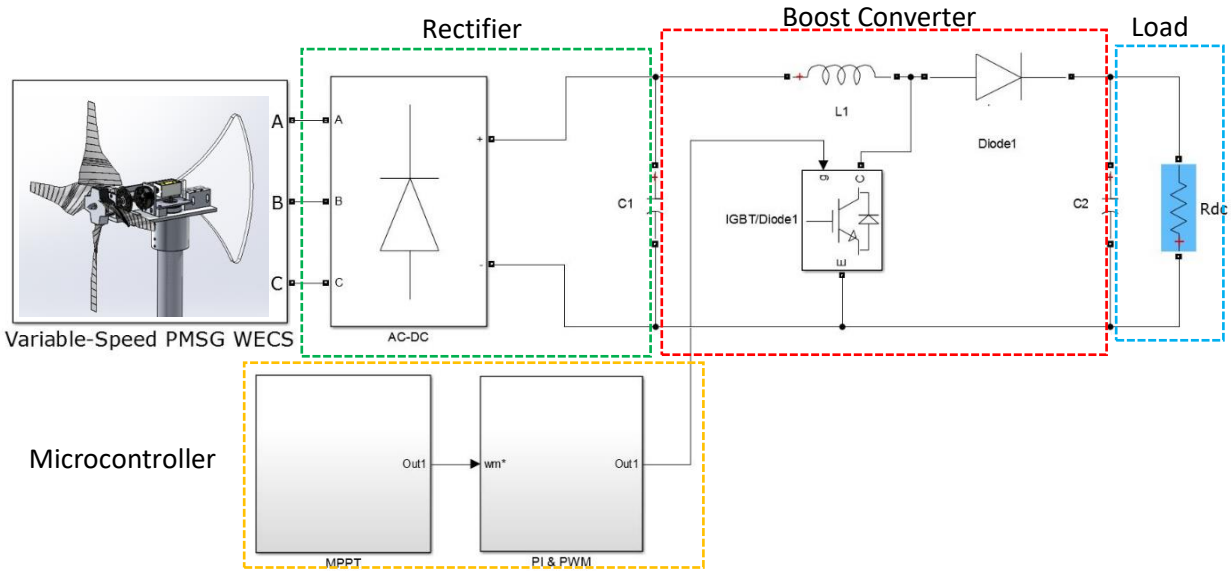

Figure 10: Power Converter Topology

2.7 Controls Analysis and Software Documentation

Simulations of various boost converters, diode bridge rectifiers, and control schemes were conducted using MATLAB's Simulink software. The simulations included multiple PI controllers as well as capacitor and inductor values to gain an overall understanding of the basic turbine, rectifier, boost converter and load design. The first simulation was comprised of a variable speed permanent magnet synchronous generator, a six-diode diode bridge rectifier, and a boost converter with an IGBT that is controlled with optimal tip speed ratio control. The circuit was connected to a resistive load to focus on the individual circuit elements and PI controller tuning. The overall boost converter topology, including smoothing capacitors, can be seen in Figure 11.

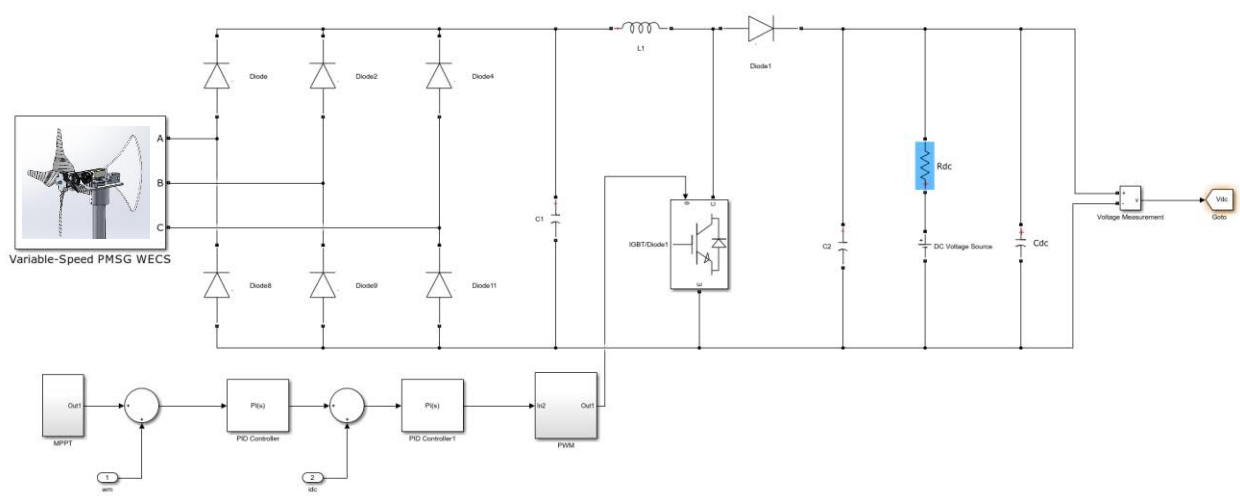

Figure 11: Boost Converter Topology

After completing the first simulation and thoroughly testing it, two simulations were developed for ABC/αß and ABC/dq control to invert the DC-DC Converter output for regulated grid-controlled power. The ABC/αß and ABC/dq control simulations were connected to a DC power supply, a two-level voltage source converter and an RL load. These conditions were chosen because of their simplicity both in construction as well as within the simulation. **The only difference between the two simulations was the calculation block for the conversion from one reference frame to the other; the two were otherwise identical.** The topology was tested for the observed current from the load to the reference current, the three-phase voltage, natural voltage and line-to-line voltage. The low-level block diagram can be seen in Figure 12.

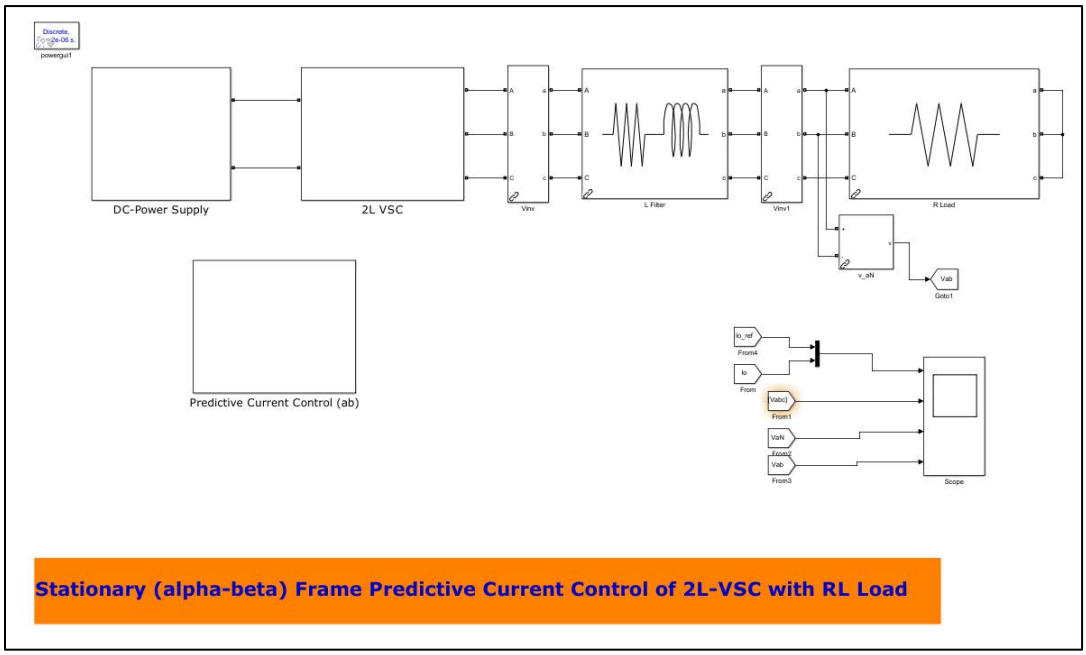

Figure 12: High Level block diagram for ABC/αß control

A similar circuit was constructed for the standalone application at the competition. The design for this circuit includes electrical and mechanical brakes and dependencies and connections for the system and its controllers. The electrical one-line diagram seen in Figure 13 contains these components and displays their purpose regarding the entire system.

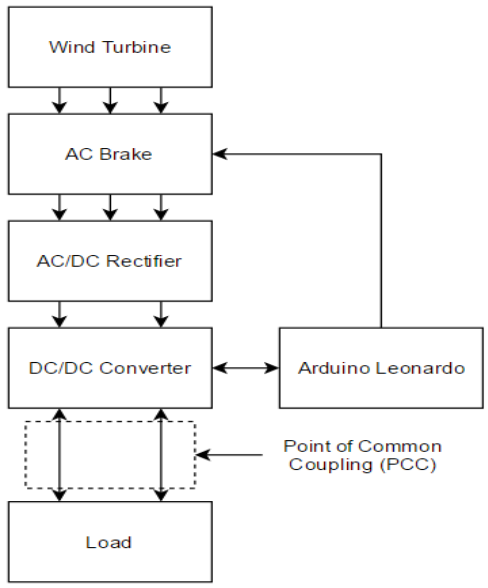

Figure 13: Electrical One-Line Diagram

Following integrated testing of purchased components, the microcontroller was programmed to determine the variable duty cycle for the switching component. The microcontroller algorithm Proportional Integral (PI) controllers and pulse width modulation (PWM) is summarized in Figure 14.

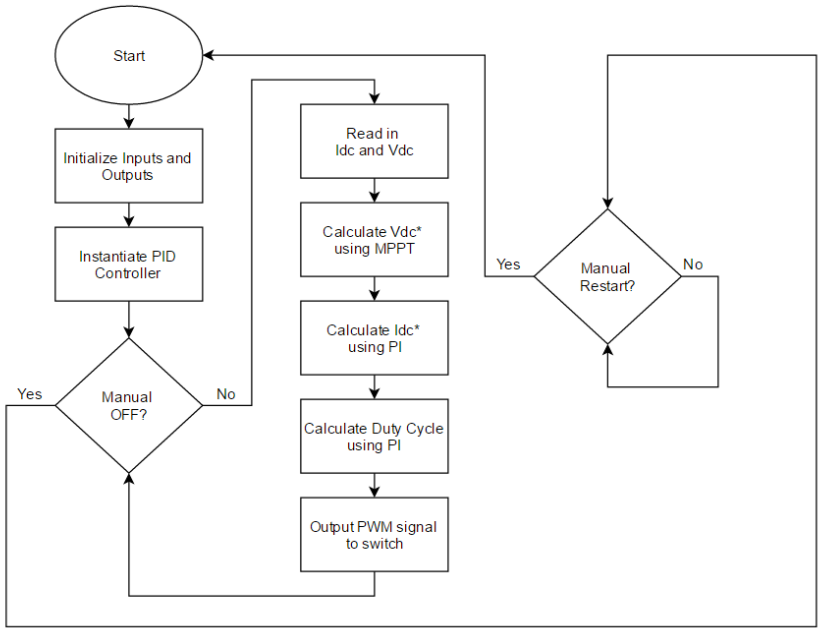

Figure 14: Control State Flow Chart

Development of a three-channel boost converter simulation was attempted; however, it was rejected when the team began development of the single-channel boost converter due to budget and time constraints. If the team is unable to produce a working DC-DC converter, the team will default to one of the purchased off-the-shelf converters for use during the competition.

2.8 Testing

2.8.1 Testing Results

The mechanical brakes were tested on a pass fail basis for functionality. The tests consisted of observing the successful actuation of the brakes by switch and actuation by disconnection from the load. Figure **15** shows the breadboard that was used for prototyping, with a latching solenoid and Arduino Nano. The latching solenoid has a permanent magnet to counteract the force of the return spring to keep the brake caliper in an open position. Once released the return spring provides the force to brake the turbine effectively. The spring constants of different springs were analyzed on how much counteractive force they can provide to the turbine assembly. The Arduino Nano is used to measure voltage drop across a shunt resistor and relate the value to the current drop once the turbine is disconnected from the load and signal the turbine to brake. The AC brakes will be used alongside the solenoid to provide the braking force to control the rpms of the driveshaft.

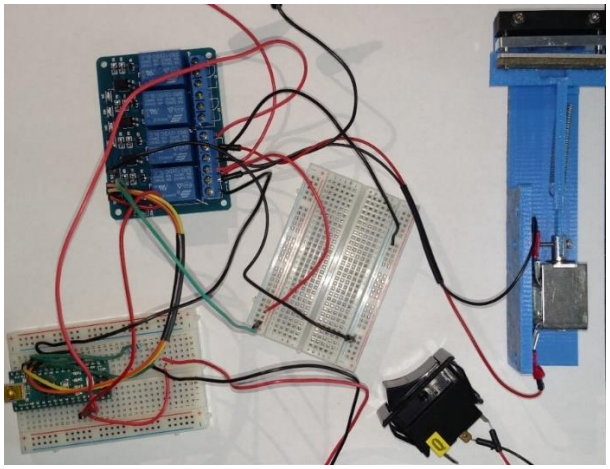

Figure 15*: Mechanical Braking System*

2.8.2 Testing Plans

Future field testing at the wind tunnel will be split into three major tests to evaluate the three critical mechanical components of the turbine: yaw, blades, and brakes. The objective is to evaluate each subsystem based on the established design criteria.

The blades will be tested by measuring cut-in speed, power output, and structural integrity. Blades will be tested for power output performance by generating and recording power curves for wind speeds from 5m/s to 11m/s increasing by 1m/s. Wind speeds from 1-5m/s will be tested to determine when the turbine begins to generate power. The power performance of the blades will solidify the operating voltage of the turbine with test values of 6V, 9V or 12V.

The brakes will be tested for actuation and braking time at various wind speeds. The mechanical brakes will first be empirically tested on a pass/fail basis based on successful actuation of the brakes by switch and disconnection from the load. The second test will be to determine the braking time intervals at different wind speeds up to 18m/s.

The yaw system will be tested at varying angles to determine if the system can efficiently rotate the turbine into the direction of the wind. The yaw system will be tested for wind tracking response time for the wind turbine to fully orient itself into the wind. The yaw system and tower will be evaluated at integral wind speeds up to 18 m/s to determine if the turbine performs safely for any wind speed and maximum vibrational loads.

3 References

[1] J. Manwell, *Wind Energy Explained*. New York: John Wiley 2001

[2] Michael Ching Kwei Kang, "Wind Turbine Blade Automatic Pitch Control using Centrifugal Force," U.S. Patent 20120141267 A1, Abbrev. June 7 2012

[3] R. Budynas and J Nisbett, *Shigley's Mechanical Engineering Design 10th Edition.* New York: McGraw-Hill 2015

[4] Oak Ridge National Laboratory, "Basic Properties of Reference Crossply Carbon-Fiber Composite," Lockheed Marting, February 2000, [Online]. Available: http://web.ornl.gov/~webworks/cpr/v823/rpt/106099.pdf

[5] ASM International, "Contact Fatigue", Transportation.org, [Online] Available: http://highways.transportation.org/documents/sec06-lts-5trev.pdf

[6] MatWeb Material Property Data, "ASTM A36 Steel Bar", [Online] Available: http://www.matweb.com/search/datasheet.aspx?matguid=d1844977c5c8440cb9a3a967f8909c3a&ckck=1

[7] J. Schon, "Coefficient of Friction for Aluminum in Contact with Carbon Fiber Epoxy Composite", February 2004, [Online] Available: http://www.sciencedirect.com/science/article/pii/S0301679X03002305

[8] "Deep groove ball bearings 61909"Internet: http://www.skf.com/us/products/bearings-units-housings/ball-bearings/deep-groove-ball-bearings/deep-groove-ball-bearings/index.html?designation=61909, [Nov. 18, 2016].

[9] "Bearing Loads" Internet: http://www.skf.com/group/products/bearings-units-housings/engineered-products/insocoat-bearings/insocoat-deep-groove-ball-bearings/loads/index.html, [Nov. 18, 2016].

[10] "SUNNYSKY." Internet: http://www.hobby-wing.com/sunnysky-x4108s-multicopter-brushless-motor.html, 2006 [Nov. 18, 2016].

[11] "Cheap Slip Rings." Internet: http://www.dxsoul.com/product/wind-turbine-6-wire-5a-per-circuit-electrical-slip-ring-for-wind-power-generation-system-901390064#specifications-detailinfo, 2006 [Nov. 18, 2016].

[12] "1/5 Baja 5B Disc Brake." Internet: http://www.dollarhobbyz.com/collections/disc-brake-parts/products/hpi-1-5-baja-5b-disc-brake-set-aluminum-rear-upper-plate, [Nov. 18, 2016].

[13] D. Wood, Small wind turbines, 1st ed. New York: Springer, 2011, pp. 145-166.

[14] "Estimating the frictional moment", Skf.com, 2016. [Online]. Available: http://www.skf.com/us/products/bearings-units-housings/ball-bearings/principles/friction/estimating-frictional-moment/index.html. [Accessed: 13- Nov- 2016].

[15] "Wind Velocity and Wind Load", Engineeringtoolbox.com, 2016. [Online]. Available: http://www.engineeringtoolbox.com/wind-load-d_1775.html. [Accessed: 17- Nov- 2016].

4 Appendix A: Exploded View-Mainframe, Tower, Tail, and Yaw System

ITEM NO.	PART NUMBER	QTY.
1	Motor Stator	1
2	Motor Rotor	1
3	Block	1
4	Mainframe	1
5	Mount	1
6	Vane Mount	2
7	Riser Block	1
8	Motor Plate	1
9	Yaw Bearing Flange	1
10	Tower Base	1
11	Slip Stator	1
12	Slip Rotor	1
13	Yaw Bearing	2
14	Bearing Spacer	1
15	Tower Shaft	1
16	Tail Vane	1
17	M6x1.0 (20mmx 5, 30mmx1, 40mmx9)	15
18	M6x1.0 Nut	14
19	M5x1.0 (10mmx2, 15mmx6)	8
20	M5x1.0 Nut	2

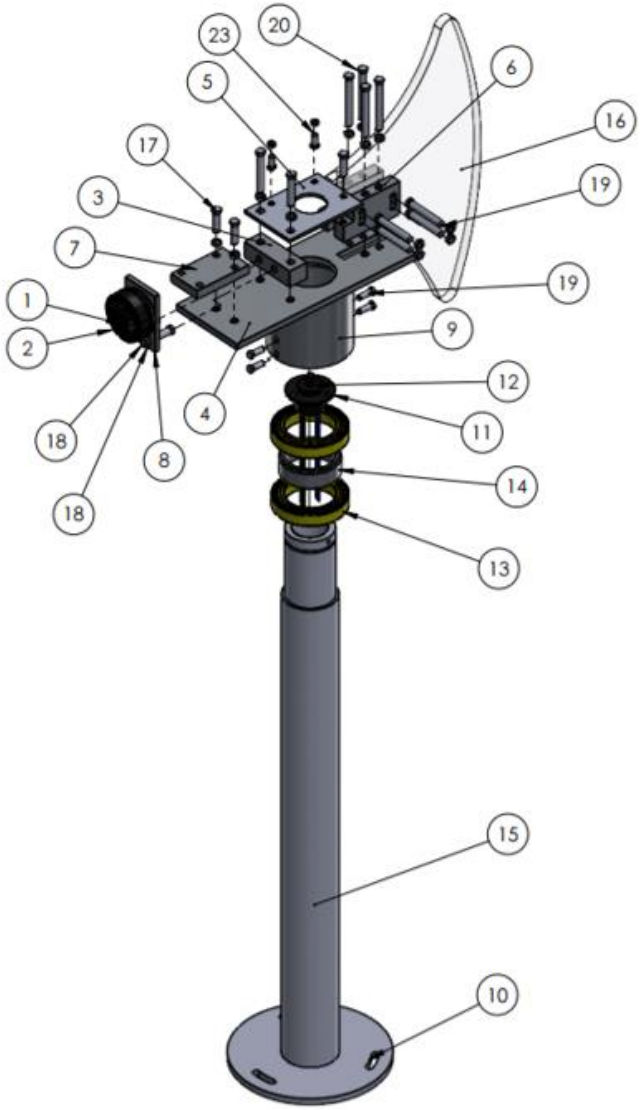

5 Appendix B: Exploded View-Hub, Brakes, Drivetrain

ITEM NO.	PART NAME	QTY.
1	BrakeRotor	1
2	Drive Shaft	1
3	Stub Shaft	1
4	Brake Hub	1
5	Motor Stator	1
6	Moter Rotor	1
7	Flange Mount, Self Align, Needle Roller Bearing	1
8	Bearing Plate	1
9	Solenoid	1
10	Plunger	1
11	Spring	1
12	Mount 2	1
13	Caliper	1
14	Pin	2
15	Shoe 2	1
16	Shoe 1	1
17	Arm	1
18	Hub Base	1
19	Hub Top	1
20	Blades	4
21	Nosecone	1
22	M3x0.8	12
23	M6x1.0 (10mm x 2, 20mmx 2, 40mm x 1)	5
24	M6x1.0Nut	5
25	M5x1.0 10mm	2
26	M5x1.0 Nut	2
28	M3x0.8 Nut	2

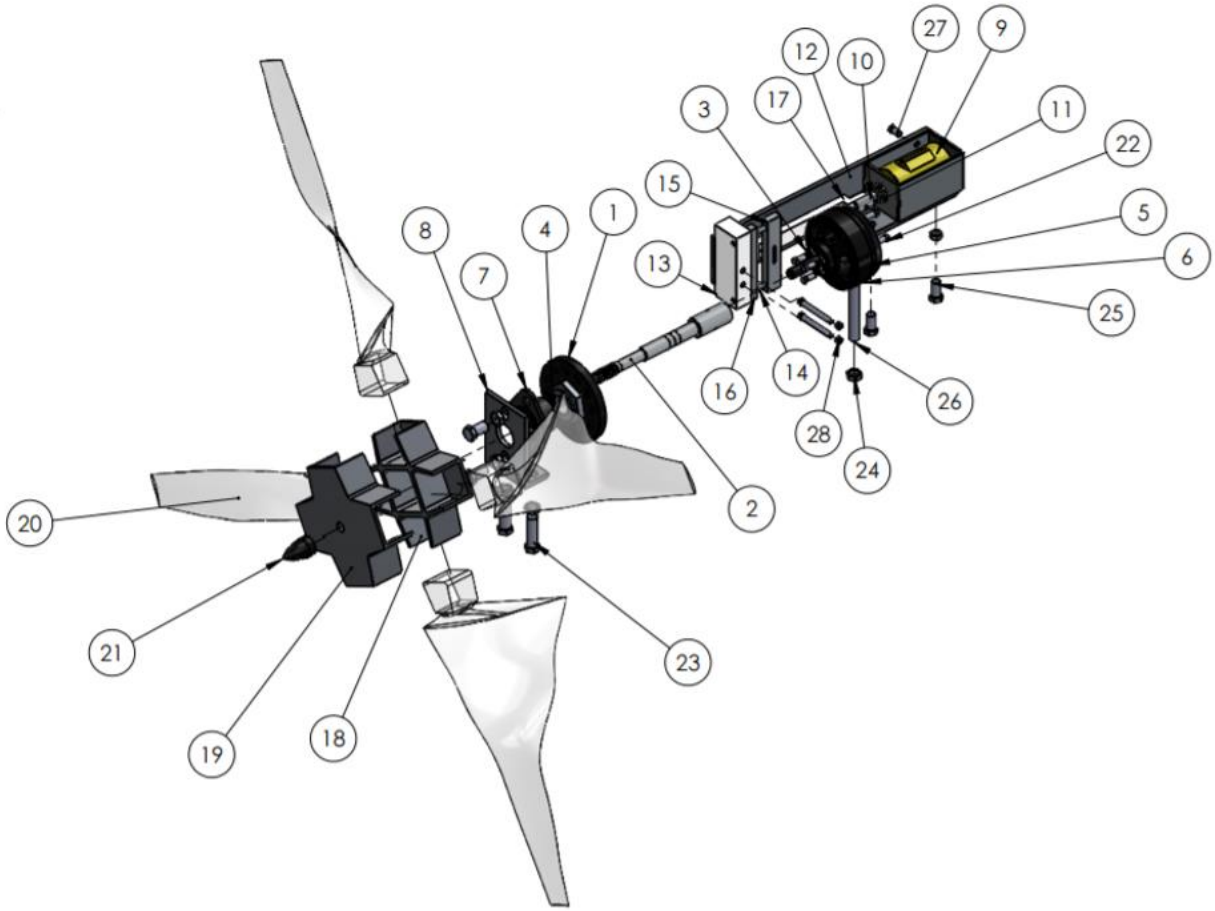

6 Appendix C: Shaft Analysis MATLAB Program, DE-Gerber Failure Criteria

```
%% Rafeal Vera Jr. Last Updated 3-28-17
%% This program is used to solve for the factors of safety for fatigue using
%the DE-Gerber failure criteria and also checks for static loading factor of safety
%use in conjunction with Shigley's Mechanical Engineering Design
%% User Inputs
diameters = input('Enter the diameter at location of interest in mm:\n'); %Diameter of
interest
Sut = input('Enter material ultimate tensile strength in MPA for shaft (pg 1048+)\n')
; %tensile strength input
Sy = input('Enter material yield strength in MPa\n'); %yield strength input for factor
of safety
%% Material Yield Stresses
Sep = Sut * .5; % Se' for Sut less than 200 kpsi or 1400 MPa
a = (4.51);  % Surface mod constant for CD or machined steel or aluminum 4.51 for MPa
2.7 for Kpsi
b = -0.265; % Surface mod constant for CD or machined steel or aluminum
ka = a * ((Sut)^b); %surface mod factor
kb = (1.24) * (diameters^-0.107);  % for inches :(0.879) * (diameters^-0.);
%kc = 1; %Because loading is in bending
Se = ka*kb*Sep;
% rod = .15; % fillet radius vs diameter ratio    larger means safer
%% Dynamic Loads
Momenta = input('Enter the alternating bending moment (Ma) at location of interest in
N-mm\n');
Torquem = input('Enter the Mean Torque (Tm) at location of interest in N-mm\n'); %Mean
Torque Through Shaft
%% Stress Geometry and Material Factors
kt  = input('Select an Kt Bend from(A-15-9) pg 1036 \n'); %kt = 2.14 and kts = 3.0 for
keyway groove
kts = input('Select an Kts tors from(A-15-8) pg 1038 \n');
q = input('Enter a value for q (notch sens) from handout or pg 303 \n'); % your gonna
need Sut
qs = input('Enter a value for qs (shear notch sense) from handout or pg 304 \n');
%% Stress Concentration Modification
kf = 1 + (q * (kt-1 )); %kt = 2.14 and kts = 3.0 for keyway groove
kfs = 1 + (qs * (kts-1 )); %surface/stress concentrator modification factors
%% De-Gerber Criteria
A = sqrt(4*((kf*Momenta)^2));
B = sqrt(3*((kfs*Torquem)^2));

ns = 1/(((8*A)/(pi*Se*diameters^3))*(1+(1+[(2*B*Se)/(A*Sut)]^2)^(1/2))); %DE-Gerber
Failure Theory: fatigue
sigprimax = sqrt (( ((32*kf*Momenta)/ (pi * diameters^3))^(2) + (3*(((16*kfs*Torquem)/
(pi * diameters^3)))^(2)) ));
ny = Sy / sigprimax;  %factor of saftey for static yield failure
nd = 1.1;
newdiameter = ( (8*nd*sqrt(4*(kf*Momenta)^2))/(pi*Se))
*(1+[1+[(2*Se*sqrt(3*(kfs*Torquem)^2))/(Sut*sqrt(4*(kf*Momenta)^2))]^2]^(1/2))^(1/3);

fprintf('Factor of saftey for fatigue is : %.4f \n' ,ns);
fprintf('Factor of saftey for yield is : %.4f \n' ,ny);
fprintf('The new diamter should be : %.4f \n' ,newdiameter);
```

7 Appendix D: Equations

Dynamics Equations:

Newton's Second Law: $F = ma_n$

Normal Acceleration: $a_n = (R_o - R_i)\omega^2$

Revolutions per Minute: $n = \frac{60\ U\ \lambda}{\pi\ D}$

Angular Velocity: $\omega = \frac{2\pi\ RPM}{60}$

Torque Coefficient: $C_Q = \frac{C_p}{\lambda}$

Rotor Torque: $Q = C_Q \frac{1}{2}\ \rho\pi R^2 U^2$ [1]

Fatigue and Yield Equations:

DE-Gerber Failure Criteria: $\frac{1}{n_f} = \frac{8A}{\pi d^3 S_e}\left\{1 + \left[1 + \left(\frac{2BS_e}{AS_{ut}}\right)^2\right]^{1/2}\right\}$

Where: $A = \sqrt{4(K_f M_a)^2}$ *and* $B = \sqrt{3(K_{fs} T_m)^2}$

Von Misses Static Yield Criteria: $n_y = \frac{S_y}{\sigma'_{max}}$

Loading is Fully Reversed therefore: $M_m, T_a = 0$

S_e , S_y , σ'_{max} *and* S_{ut} *are calculated using material properties and modification factors from Shigley's [3] and are omitted in this report*

Uniform Pressure Criteria (Brake) Equations:

Braking Force, New Brakes: $F = \frac{1}{2}(\theta_2 - \theta_1)p_a(r_o^2 - r_i^2)$

Resistive Torque: $Q = \frac{1}{3}(\theta_2 - \theta_1)f p_a(r_o^3 - r_i^3)$

8 Appendix E: Assumptions and Material Properties

Dynamics Assumptions:

Angular Velocity is Constant ω = constant, Tangential Acceleration is zero, $a_t = 0$

Blade Radius, Hub Radius and Total Rotor Diameter, R_B = .20 m, R_H = .02 m and D = .44 m

PLA Blade and Aluminum Hub Mass, m_B = 0.022 kg/blade, m_H = 0.022 kg/arm

Golden, Colorado Air Density, $\rho = 1.324\ kg/m^3$

Tip Speed Ratio, λ = 4 (for maximum torque)

Average Coefficient of Performance, $C_p = 0.500$ (for maximum torque)

Brake Assumptions

Theta is Brake Pad Span in Radians: θ_1= 0.523 and θ_2= 2.617

Inner and Outer Brake Pad Radii are: r_i= 14 mm and r_o= 22 mm

The Pads are assumed to be Annular (Curved)

Material Properties:

6061-T6 Aluminum: S_{ut}= 310 MPa ,S_y= 276 MPa

7075-T6 Aluminum: S_{ut}= 593 MPa, S_y= 542 MPa

VEROCLEAR 3D Filament: S_y= 50MPa

Brake Pads are T6-6061 Aluminum with Max Contact Pressure of: 241MPa [5]

The Brake Disk is Carbon Fiber ($\pm$45° fiber orientation) with Max Contact Pressure of: 163 MPa [4]

Max Contact Pressure of Steel (for Estimation Purposes) is: 152MPa [6]

Max Contact Pressure of Carbon Graphite on Steel (for Estimation Purposes) is: 2.10 MPa [3]

Coefficient of Friction of CF-AL Ranges from: f=0.23-0.68, Estimated at f= 0.37 [7]

Estimated Max Pressure for CF-AL Interface: 2.50 MPa